JOURNAL OF NEUROTRAUMA 30:840–852 (May 15, 2013)

DOI: 10.1089/neu.2012.2670

Intravenous Infusion of Magnesium Chloride Improves Epicenter Blood Flow during the Acute Stage of Contusive Spinal Cord Injury in Rats

Johongir M. Muradov[1,2] and Theo Hagg[1–3]

Abstract

Vasospasm, hemorrhage, and loss of microvessels at the site of contusive or compressive spinal cord injury lead to infarction and initiate secondary degeneration. Here, we used intravenous injection of endothelial-binding lectin followed by histology to show that the number of perfused microvessels at the injury site is decreased by 80–90% as early as 20 min following a moderate T9 contusion in adult female rats. Hemorrhage within the spinal cord also was maximal at 20 min, consistent with its vasoconstrictive actions in the central nervous system (CNS). Microvascular blood flow recovered to up to 50% of normal volume in the injury penumbra by 6 h, but not at the epicenter. A comparison with an endothelial cell marker suggested that many microvessels fail to be reperfused up to 48 h post-injury. The ischemia was probably caused by vasospasm of vessels penetrating the parenchyma, because repeated Doppler measurements over the spinal cord showed a doubling of total blood flow over the first 12 h. Moreover, intravenous infusion of magnesium chloride, used clinically to treat CNS vasospasm, greatly improved the number of perfused microvessels at 24 and 48 h. The magnesium treatment seemed safe as it did not increase hemorrhage, despite the improved parenchymal blood flow. However, the treatment did not reduce acute microvessel, motor neuron or oligodendrocyte loss, and when infused for 7 days did not affect functional recovery or spared epicenter white matter over a 4 week period. These data suggest that microvascular blood flow can be restored with a clinically relevant treatment following spinal cord injury.

Key words: blood flow; capillaries; contusion; hemorrhage; vasospasm

Introduction

Contusive or compressive spinal cord injuries (SCI) initiate a pathological cascade starting with hemorrhage and microvascular dysfunction.[1–4] Early vasospasm, including that of the pial vessels, causes ischemia in rats and cats as identified by microangiography and hydrogen clearance measurements.[5–7] SCI also results in hemorrhage caused by microvascular disturbances and results in secondary hemorrhagic necrosis.[8–10] Hemorrhage induces vasospasm after subarachnoid hemorrhage. The central nervous system (CNS) vasodilator nimodipine can increase global spinal cord blood flow and rescue electrophysiological conduction in rats during the acute phase, if blood pressure is maintained,[11,12] but does not provide permanent benefits.[13] Also, nimodipine was not found to be beneficial in a small clinical series of human SCI patients, although these were likely underpowered to show a clinical effect, if any.[14] Currently, in the United States, nimodipine can only be given orally, which most likely reduces the rapid bioavailability needed for neuroprotection following acute SCI.

Intravenous infusion of magnesium is one of the options in the treatment of human cerebral vasospasm.[15,16] Magnesium treatment has not been tested in humans with SCI. In rats, two intravenous injections of magnesium at 15 min and 6 h following a clip compression injury resulted in white matter sparing dorsally to and at the injury epicenter, with improved locomotor function over 6 weeks.[17] However, after a contusive injury, such a treatment reduced the lesion volume but did not improve locomotor function.[18] Those studies did not assess the vasodilatory effects, as they were aimed at utilizing magnesium's ability to reduce cytotoxic mechanisms, including glutamate toxicity.[19] Therefore, it is possible that because of a high excretion rate of magnesium, the intermittent treatments did not reduce the vasospasm and hypoperfusion, and that continuous intravenous magnesium infusion would have been more efficacious. Also, it remains to be determined whether magnesium treatment might exacerbate the injury-induced hemorrhage, which could counteract its protective effects following SCI.

We previously found that protection of perfused blood microvessels and their endothelial cells within the spinal cord over the 1st week following contusive SCI greatly improved white matter

[1]Kentucky Spinal Cord Injury Research Center and Departments of [2]Neurological Surgery and [3]Pharmacology and Toxicology, University of Louisville, Louisville, Kentucky.

sparing and locomotor function in rats and mice.[20,21] Endothelial cell loss might be caused by pathological calcium influx or lipid peroxidation, which can be reduced by magnesium treatment in brain injury.[19,22,23] It remains to be determined whether microvascular endothelial cells can be protected following resolution of vasospasm, as reperfusion injury might be detrimental following SCI.[24] We and others identify perfused microvessels by intravenous injection of the lectin, *Lycopersicon esculentum* (tomato) agglutinin (LEA), which binds to glucosamines on endothelial cells.[25–28] Microscopic histological analyses of LEA+ microvessels provide a measure of the perfusion status of microvessels that are lined with endothelial cells at the injury epicenter and penumbra, two areas where therapeutic intervention is needed during the acute stage of injury.[20,21,29]

Here, we determined the temporal changes in the number of perfused and endothelial-lined microvasculature over 2 days following contusive SCI in adult rats. We also tested continuous intravenous magnesium infusion to improve blood flow and survival of endothelial cells in the injury epicenter and penumbra, and potential exacerbating effects on hemorrhage. Finally, we determined whether magnesium infusion during the 1st week would provide lasting improvements in white matter sparing and locomotor function.

Methods

Animals and experimental design

Seventy-eight young adult female Sprague Dawley rats were used (180–220 g; Harlan; Table 1). We first determined the time course of vascular changes between 20 min and 48 h following a contusive SCI. A second experiment determined the effects of intravenous infusions of magnesium over a 24 or 48 h period. Third, we tested whether a 7 day magnesium infusion would be neuroprotective and improve locomotor function over 4 weeks. All animal procedures were conducted according to the guidelines of National Institutes of Health, and were approved by the University of Louisville Institutional Animal Care and Use Committee. Animals were allowed to habituate to their cages for at least 48 h after arrival, and had free access to food and water. Investigators involved in surgeries, behavioral testing, and quantification of histological results were blinded to the treatment group.

SCI

All invasive procedures were conducted with the animals under deep anesthesia with an intramuscular injection of a 3.3 mL/kg mixture containing 25 mg/mL ketamine hydrochloride (Abbott Laboratories, Abbott Park, IL), 1.2 mg/mL acepromazine maleate (The Butler Company, Dublin, OH), and 0.25 mg/mL xylazine (The Butler Company) in 0.9% saline. Animals received a subcutaneous injection of 5 mL of saline for rehydration, eye protective ointment (Rugby Laboratories, Duluth, GA), and an intramuscular injection of 0.1 mL of a 100 μg/mL stock solution of gentamicin (Butler-Schein, Dublin, OH) to reduce infections.

All surgeries were performed under aseptic conditions and under visualization with a Wild M695 motorized surgical microscope. After a dorsal skin incision and soft tissue dissection at the T8-T10 level, the T9 vertebra was stabilized in a frame with steel clamps inserted under the transverse processes. Laminectomy was performed without opening the dura. The spinal cord was contused using an Infinite Horizons (IH) impactor (Precision Systems and Instrumentation, Lexington, KY) set at 150 kdyn with a 2.5 mm diameter impactor tip. Afterwards, the muscles were sutured with 5.0 silk and the skin was held with 9 mm metal clips (Braintree, ACS-cs, Braintree, MA). Bacitracin ointment (Qualitest Pharmaceuticals, Huntsville, AL) was applied to the wound to reduce infections, and another 5 mL of normal saline solution was injected subcutaneously. The animals were allowed to recover on a water-circulating heating pad at 37°C (Gaymar Industries, Orchard Park, NY). Sham-operated animals received only a laminectomy. Postoperative care included twice daily bladder expression.

Spinal cord laser Doppler measurements

To measure spinal cord blood flow we used Doppler laser measurements in four rats with a Moor VMS-LDF1 device (Moor instruments Inc., Wilmington, DE) with a VP10M200ST master probe connected to a P10D plastic fiber (outer diameter 0.5 mm). After vertebral stabilization and a T9 laminectomy, the probe was placed ~1 mm above the cord, close to the rostral end of laminectomy window, which was covered with a layer of lucent water-based gel (Surgilube, Fougera & Co, Melville, NY). The laser beam covered an area of 1 mm^2 and penetrated up to 1 mm into the tissue, thus covering more than half of the depth of cord and obtaining readings from the superficial vessels as well as much of the gray matter where microvascular perfusion is most abundant. Ten baseline readings were obtained before the contusion injury. Afterwards, the probe was removed and a 150 kdyn force injury was performed as described previously. Spinal cord blood flow was repeatedly measured in each animal at various times between 1 min and 48 h after the injury, positioning the laser Doppler probe to the initial measurement area. The bony edge of the laminectomy window was used as a reference point to ensure the same position of the optic probe in repetitive measurements. For measurements at intervals > 1 h, animals were anesthetized with Isoflurane (Butler, Dublin, OH). An average of 10 readings at each given time point was calculated for each animal, and expressed as a percentage of baseline readings.

Continuous intravenous infusions

Animals received a continuous intravenous infusion of phosphate-buffered saline (PBS) or $MgCl_2$ (31 mg/day = 155 mg/kg/day

Table 1. Experimental Design

Experiment (all after T9 contusion)	*Survival period*	*Treatment*	*No. rats*
1 Temporal profile of microvascular changes	Sham control	None	8
	20 min, 1, 3, 6, 12, 24, 48 h	None	5 each time point
2 Laser Doppler study of spinal cord blood flow	48 h	None	4
3 Effect of intravenous infusion of $MgCl_2$	24 or 48 h	PBS	5 each time point
on microvasculature	24 or 48 h	$MgCl_2$	5 each time point
4 Effect of 7 day $MgCl_2$ infusion on locomotor	4 weeks	PBS	6
function and tissue sparing		$MgCl_2$	5

PBS, phosphate-buffered saline.

in ddH_2O; Cat #M2670; Sigma, St. Louis, MO). Earlier studies had used the magnesium sulfate form by itself.[17,18] However, because of slightly better outcomes after $MgCl_2$ than after magnesium sulfate in combinations with polyethylene glycol following a contusion injury, $MgCl_2$ had been chosen for further optimization and characterization (combined with polyethylene glycol).[18,30] Therefore, we chose to test $MgCl_2$. Both the chloride and sulfate forms are used clinically. The daily dose of 760 μmol/kg was extrapolated from a previous study in which 190 μmol/kg per intravenous injection was deemed effective and in line with tolerable doses in humans, and a 6 h interval (four injections per 24 h) protected most tissue.[18] This dose also showed efficacy when combined with polyethylene glycol.[18,30] Alzet pumps (model 2001D for 24 h, model 1003D for 48 h, and model 2001 for 7 days; Alzet Corporation, Cupertino, CA) were primed overnight in saline with their openings facing upwards to prevent inflow of saline, and then filled with reagent. Intravenous catheters were custom made from polyurethane intravascular tubing (1.2 mm outer diameter, 0.69 mm inner diameter; cat # PY2 72-4431; Harvard Apparatus, Holliston, MA) pulled over an open flame to a 100 μm diameter over 3 mm and then gas-sterilized. They were also filled and connected to the pumps through their flow moderators, which were inserted all but 2 mm into the pump. Immediately after the SCI, the right jugular vein was exposed by blunt dissection after a skin incision in the anterolateral neck area. A subcutaneous tunnel was made by blunt dissection to the posterior-lateral cervical and posterior thoracic area for placement of the pump that was attached to the thick end of the catheter. Two ligatures were placed around the mid-cervical portion of the jugular vein. The more rostral ligature was gently retracted to stop blood flow while the caudal one was tightened, but leaving the vessel lumen open. A small (0.5 mm) hole was made in between two ligatures with microscissors, and the catheter tip was inserted into the vein to a 10–12 mm depth. The caudal ligature was tightened around the vein and catheter. Next, the flow moderator was inserted all the way into the pump to expel any potential blood from the catheter tip. The rostral ligature was tightened and secured the catheter to adjacent soft tissues. The wounds were sutured in layers. The patency of the infusions was confirmed by checking that the catheter tip was positioned correctly within the jugular vein lumen and by checking that almost no solution remained within the Alzet pump after the rats were euthanized.

Functional assessments

All animals in the 4 week experiment were tested for overground locomotor performance at weekly intervals. To reduce stress and inter-animal variability, they were handled over a period of 3 days and allowed to adapt to the test devices before testing. Open field locomotor function was performed using the Basso–Beattie–Breshnahan (BBB) scale.[31] Once a rat walked continuously in the open field (circular tub), two certified examiners scored the performance for 4 min. Baseline values were obtained on the day before surgery. Animals were tested on the 2nd day to ensure equal injury severities between groups and weekly, starting at 7 days post-injury. The rats were also tested in a sensorimotor grid walk test, which is particularly sensitive to dorsal column injury.[20] Rats walked voluntarily on a 114×114 cm grid with 3.8 cm holes. The number of hindlimb footfalls were counted by two observers from different sides and recorded by a third person. The test was terminated after total 90 sec of walking was observed, and the total time of the test was recorded. Baseline values were determined on the day before injury.

Histological procedures

Depending upon the experiment, animals survived between 20 min and 4 weeks after the spinal cord contusion. Twenty minutes prior to processing for histology, the left jugular vein was exposed and 200 μL containing 200 μg rhodamine-conjugated LEA (Vector Laboratories, Burlingame, CA) was injected over 1 min. After 20 min, the rats were perfused with 200 mL ice-cold 0.1 M PBS followed by 200 mL 4% paraformaldehyde (PFA; Cat #19210; Sigma, St. Louis, MO) in phosphate buffer. The block of thoracic spine was excised and post-fixed overnight in PFA before dissection of the spinal cord, which was affixed to a strip of dental wax to straighten it, and cryoprotected in 30% sucrose overnight. A segment of 11 mm containing the injury epicenter in the center was collected. Multiple spinal cords were aligned and a reference tissue to orient each batch were cast in a single block of Tissue Freezing Medium (TMF-5, Triangle Biomedical Sciences Inc., Durham, NC) and frozen at -20°C. Every other 20 μm transverse section was collected on a cryostat onto SuperFrost plus glass slides (VWR, Radnor, PA) to produce five series with each section separated by 200 μm.

Before staining, slides containing the transverse sections were warmed and dried at 37°C for 60 min, and the freezing medium was removed. All other steps were at room temperature. Sections were incubated flat, and a wall was drawn with a slide marker (RPI, Mount Prospect, IL) around the edges of the slide to retain fluids. The slides were washed with PBS 3 times for 10 min in between all steps. To visualize LEA, every fifth slide was processed for immunohistochemistry to amplify the LEA signal (1:500; goat anti-rhodamine immunoglobulin G [IgG]; Cat SP-0602; Vector Laboratories; Burlingame, CA) using Alexa594-conjugated donkey anti-goat secondary antibodies (1:200; Cat#A11058; Invitrogen, Grand Island, NY). The same sections were immunostained for the endothelial marker RECA1 (1:1000; mouse anti-rat monoclonal antibody; catalog #MCA970; Serotec, Raleigh, NC), combined with Alexa488-conjugated donkey anti-mouse IgG as secondary antibody (1:200; Cat#A21202; Invitrogen). Oligodendrocytes were identified with mouse anti-APC antibody; 1:1000 (Cat # OP80, Millipore, Billerica, MA), with secondary Alexa488-conjugated donkey anti-mouse IgG as secondary antibody (1:200; Cat#A21202; Invitrogen). The slides were cover-slipped with fluoromount-G (Cat# 0100-01; Southern Biotech, Birmingham, AL).

Sections adjacent to the LEA-stained sections were used to document the extent of hemorrhage using the diaminobenzidine (DAB) staining step in which endogenous peroxidases in red blood cells convert the DAB substrate.[32] Briefly, the slides were washed with PBS twice for 10 min, and then for 10 min in 0.05 M Tris buffered Hanks saline (TBH) without sodium chloride. The DAB solution was prepared fresh and contained 0.4 mg/mL DAB (Cat #D5637, Sigma, St. Louis, MO), 0.6 mg/mL ammonium nickel sulfate and 0.6 μl/mL of 30% hydrogen peroxide, all in 0.05 M TBH. Slides were incubated in DAB solution for 5 min, rinsed three times for 10 min with PBS, washed in 0.1 M PB, then serially dehydrated up to 100% ethanol followed by xylene, and then cover-slipped in Permount (SP15-500, Fisher Scientific, Pittsburg, PA).

White matter was stained with an Eriochrome Cyanine (EC) staining protocol.[33] Dried slides were immersed in xylene twice for 30 min to remove freezing medium remnants, and the sections were hydrated through a graded ethanol range up to 50%. EC solution consisted of 2 mL of 10% $FeCl_3$ (cat # 157740; Sigma) and 40 mL of 0.2% EC (cat # 32752; Sigma) in 0.5% aqueous H_2SO_4 (cat # 339741; Sigma) and brought to a final volume of 50 mL with ddH_2O). EC was applied to the slides for 10 min. The final step consisted of rinsing with ddH_2O and differentiating with 0.5% aqueous NH_4OH (cat # 221228; Sigma) for 30 sec. After termination of the reaction with a ddH_2O wash, slides were dehydrated and cover-slipped in Permount.

Adjacent sections were stained with cresyl violet (CV) to detect neuronal cell bodies. First, to clear cords from hemorrhage, slides were soaked to 3 min to 0.3% H_20_2 solution (cat # HX0635-1; EMD Chemicals; Gibbstown, NJ). Next, sections were de-fatted with graded ethanol range to 95% and rehydrated back to 50% and

ddH_2O and then placed in a 0.1% cresyl violet solution (in ddH_20; cat # C1791; Sigma) for 8 min. Sections were differentiated in 0.1% acetic acid (cat A0808; Sigma) in 95% ethanol for 30 sec, dehydrated through an ethanol range to xylene, and then cover-slipped in Permount.

Quantitative measurements and statistical analyses

Stitched (mosaic) fluorescent images of whole transverse sections were taken on a DM 6000 Leica upright microscope with a 20x objective and Surveyor software (Objective Imaging, Cambridge, UK) combined with an Oasis Automation Controller (Objective Imaging, Cambridge, UK) driving the motorized stage. All images within a type of staining were taken with the same exposure time.

LEA+ or RECA+ microvessels intersecting grid lines were counted at a high magnification. Briefly, in Adobe Photoshop CS5 software (Adobe systems, San Jose, CA), a 800×800 μm grid with a 100 μm cell size was placed over the dorsal central area between dorsal horns and over the ventral area on one side of the spinal cord using the central canal as a guide (Fig. 1I). [34] Tube-like structures were visually identified, and those intersecting the horizontal or vertical lines were counted manually. For the acute phase experiments, the injury epicenter was defined by the three sections with the lowest number of LEA+ microvessels, as determined by counts in one series of sections (each 200 μm apart) through the 11 mm length of the collected thoracic spinal cord segment. This epicenter was used as a reference point for quantifying the extent of hemorrhage, and the number of motor neurons and oligodendrocytes in adjacent series of sections. The penumbra was defined as the three sections 1 mm rostral and the three sections caudal to the epicenter. The average number of microvessels in the three sections through the epicenter, as well as the three sections in the rostral and caudal penumbrae, respectively, were calculated for each animal.[21] The average of both penumbra values for each rat were used to represent the penumbra value.

For quantification of the hemorrhagic area, gray scale images of DAB-stained sections were taken with a 10x objective and stitched

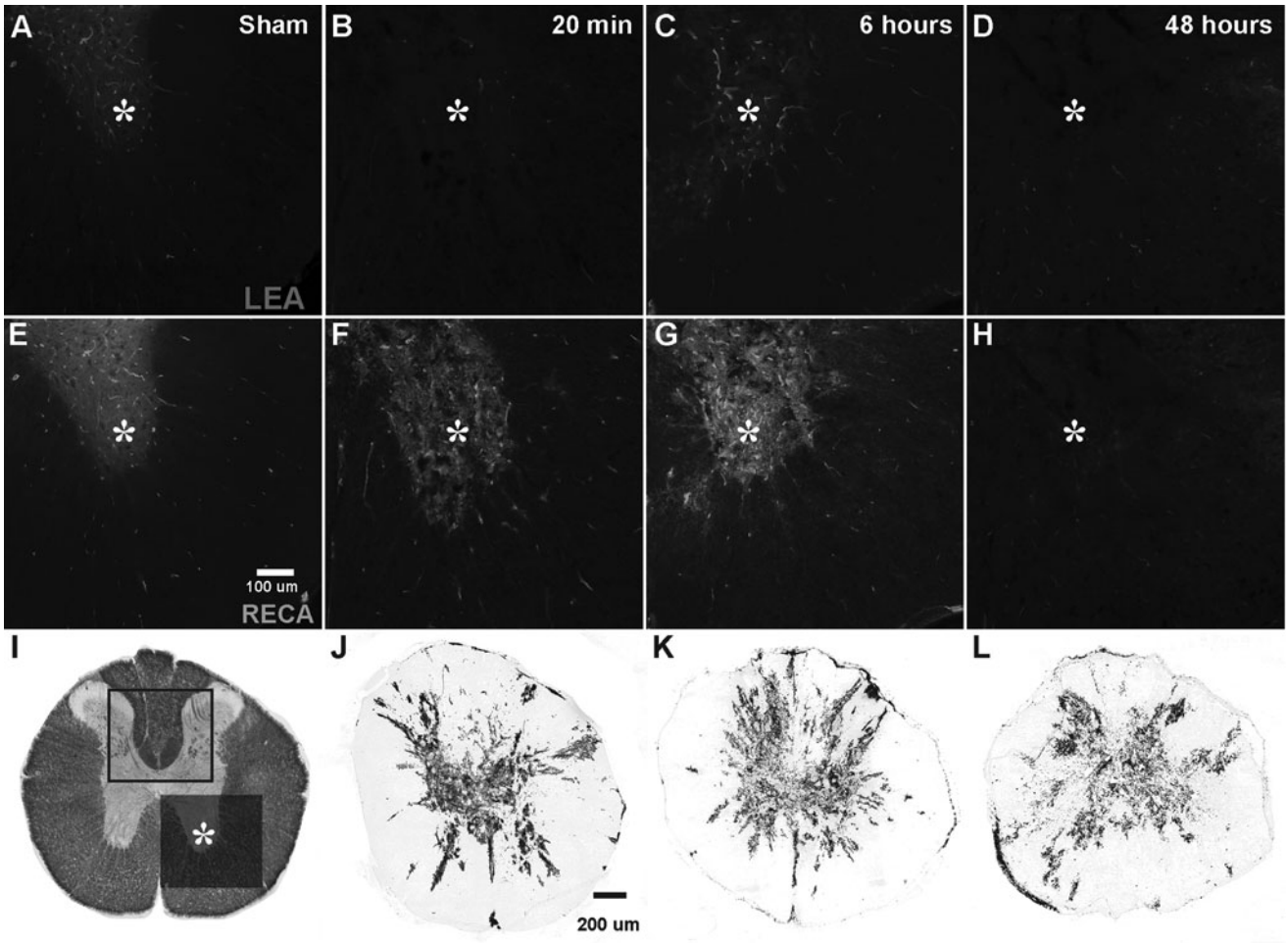

FIG. 1. Loss of tissue perfusion is rapid following spinal cord contusion. **(A–H)** are from a ventrolateral region of ventral horn (asterisk) and adjacent white matter (see darker area in **I**) in transverse sections 1 mm from the injury epicenter. **(A–D)** LEA staining. **(E–H)** RECA staining. A similar pattern of LEA- and RECA-stained microvessels is seen in gray and white matter of sham-operated rats **(A,E).** (**B,F**) Twenty minutes after the injury, the ventral horn is distorted and the number of vascular structures is decreased. **(C,G)** At 6 h, more vascular structures are detectable. **(D,H)** At 48 h post-injury, the gray matter is distorted and loss of structural integrity is evident. Note the patchy pattern of LEA- and RECA-stained vessels displaying vascular disintegration. **(I)** An Eriochrome Cyanine (EC)-stained transverse section through the normal thoracic cord showing the location of the counting grids used to quantify the microvasculature. **(J–L)** Shows the hemorrhagic area in transverse sections area at 20 min, 6 h, and 48 h post-injury. Bleeding is predominantly seen in the entire gray matter with small linear patches in the white matter. Scale bar in **E** = 100 μm for **A–H** and in **J** = 200 μm for **I–L**.

with the abovementioned microscope hardware and software. Quantification of the hemorrhage area was performed using ImageJ 1.45s software (Wayne Rasband, NIH, Bethesda, MD). The image of the whole spinal cord was transformed to a binary image, and the percentage of black pixels representing the hemorrhagic area (DAB stained) was calculated. The numbers of the three sections at the epicenter were averaged, as well as those of the three sections at 1 mm rostral and 1 mm caudal to the penumbra, for every animal. The average of both penumbra values for each rat was used to represent the penumbra value.

Motor neurons were completely absent at the epicenter or at 1 mm from it. Therefore, the number of motor neurons in the ventral horn was counted manually in three cresyl violet- stained sections at 3 mm rostral from the epicenter, and recalculated as a percentage of sham-operated controls. Oligodendrocyte cell bodies were identified by APC staining and counted manually in the white matter of the right ventral quadrant of the cord in an adjacent series of three sections at 3 mm rostral from the epicenter. This number was also recalculated as a percentage of sham controls.

For the 4 week study, images of EC-stained sections of the cord were obtained as described. Quantification of preserved white matter was performed by calculation of EC- positive pixels in one series of sections (200 μm apart) through the collected 11 mm spinal cord segment. Briefly, after the transformation of each section to a binary image, the percentage of black pixels was calculated for every section, and the average of three consecutive images was calculated. The three sections with the minimum area of EC staining were defined as the injury epicenter. The penumbra was defined as three sections 1 mm rostral and caudal to the epicenter.

In experiments with two groups, the Student *t* test was used to determine whether statistical differences existed. ANOVA with Tukey's multiple comparison's test was used to compare more than two groups. Results of the behavioral testing were analyzed by repeated measures ANOVA and by paired Student's test for each individual rat. A value of $p < 0.05$ was considered statistically significant. Microsoft Excel 2010 (Microsoft Co., San Jose, CA) was used to collect primary data and to create tables and graphs. ANOVA was performed with Prism 5 (GraphPad, La Jolla, CA). Final versions of figures were created with Adobe Illustrator software (Adobe systems, San Jose, CA).

Results

Temporal profile of microvascular perfusion in the acute stage of SCI

The distribution of the LEA+ and RECA+ microvessels in the spinal cord of sham- operated animals was the same, with a typical dense capillary network in the gray matter compared with white matter (Fig. 1A, E). At 20 min after the contusion, the injury epicenter showed signs of severe damage with almost no LEA+ microvessels in the dorsal spinal cord (not shown). In the penumbra (1 mm from the epicenter), the ventral horns had very few detectable microvessels remaining, with some present in the white matter rim (Fig. 1B). RECA staining showed a similar pattern (Fig. 1F). At 6 h, more RECA+ microvessels were seen, but not a recovery of LEA+ vessels (not shown). In the penumbra, partial recovery of LEA+ vessels was seen in both gray and white matter (Fig. 1C). However, the microvascular density was much lower compared with that in the sham-operated animals. At 48 h, LEA and RECA staining showed the disintegration of the microvascular network, more so at the epicenter (not shown) than in the penumbra (Fig. 1D,H).

The number of microvessels was determined in two regions (Fig. 1I) within the spinal cord sections, combined and expressed as a percentage of sham. At the injury epicenter, the number of LEA+ or RECA+ microvessels was reduced to $7 \pm 2\%$ or $13 \pm 4\%$, respectively, at 20 min. (Fig. 2A). The number of LEA+ epicenter microvessels did not significantly change over 48 h, when only $3 \pm 1\%$ were observed (Fig. 2A,B). At 3 h, the number of RECA+ microvessels increased up to $25 \pm 3\%$ ($p < 0.05$ vs. 1 h) and stayed constant up to 24 h, after which they declined to $9 \pm 3\%$ by 48 h ($p < 0.05$ vs. 24 h; Fig. 2A,B). The recovery of RECA may indicate protein downregulation immediately following injury, or issues with perfusion-fixation. The discrepancy between the low LEA+ and higher RECA+ ($p < 0.001$ for 12 and 24 h; $p < 0.05$ for 3, 6, and 48 h) in the epicenter suggests that most of the surviving epicenter vessels were not perfused.

In the adjacent rostral and caudal penumbra areas 1 mm away from the injury, the number of LEA+ or RECA+ microvessels was reduced to $\sim 30\%$ of sham at 20 min (Fig. 2C). This reduction persisted at 1 h, but recovered up to $55 \pm 5\%$ (LEA) and $64 \pm 10\%$ (RECA), respectively, at 6 h post-injury ($p < 0.001$; 1 vs. 6 h). This recovery continued up to 24 h, when $40 \pm 4\%$ (LEA) and $58 \pm 3\%$ (RECA) were detected (Fig. 2C,D). At the 48 h time point, the microvessels were reduced to $23 \pm 1\%$ (LEA) and $38 \pm 3\%$ (RECA)($p < 0.001$ and $p < 0.05$ vs. 6 h). The discrepancy between the LEA+ and RECA+ ($p < 0.01$) microvessels from 12 to 48 h suggests that a proportion of them were not perfused.

Temporal profile of hemorrhage in the acute stage of SCI

DAB staining was used to document the dynamics of the hemorrhagic area. Spinal cords of sham-operated animals were negative for DAB staining (not shown). At 20 min post-injury, the hemorrhagic area was predominantly located in the gray matter, and had a compact appearance (Fig. 1J). At the epicenter, the hemorrhage completely occupied the gray matter with small patches in adjacent white matter. In the penumbra, the hemorrhage was located more centrally. By 6 h, the overall area was similar to that seen at 20 min (Fig. 1K). Compared with at the earlier post-injury times, the hemorrhagic areas appeared lighter at 6 h. At 48 h post-injury (Fig. 1L), the transformation of the hemorrhagic area seemed to continue. At the epicenter, the lighter colored hemorrhagic area expanded into the white matter, reaching the dorsal outer surface. The overall density of DAB decreased, with some areas oriented radially. These changes in the compactness of hemorrhage area may be attributed to edema, heme destruction, and infiltration of inflammatory cells, which would also be stained because of their endogenous peroxidases.

The area of hemorrhage was quantified. Already at 20 min post-injury, hemorrhage was maximal at the epicenter and penumbra 1 mm away, occupying $29 \pm 3\%$ and $15 \pm 1\%$, respectively, of the spinal cord cross-sectional area (Fig. 3A). The values at the epicenter were higher than at the penumbra at most post-injury times ($p < 0.05$). The area of hemorrhage at the epicenter was lower at 24 and 48 h than at 20 min ($p < 0.01$) and 1 h ($p < 0.05$) post-injury (Fig. 3B). At the penumbra, the values were lower at 24 and 48 h than at 12 h (Fig. 3B; $p < 0.01$). This reduction might be attributed to the breakdown of heme.[9,35]

Laser Doppler flowmetry in the acute stage of SCI

Values were calculated within individual rats compared with their individual baseline readings which were considered as 100%. Acutely after injury (1 min), we observed a rapid increase up to $174 \pm 13\%$, with a further increment up to $218 \pm 10\%$ at 2 h (Fig. 3C). The flow declined to $\sim 50\%$ between 12 and 30 (Fig. 3C,D). The increase of overall flow suggests that the reduction of microvascular perfusion because of a spasm of the superficial arterioles.[36]

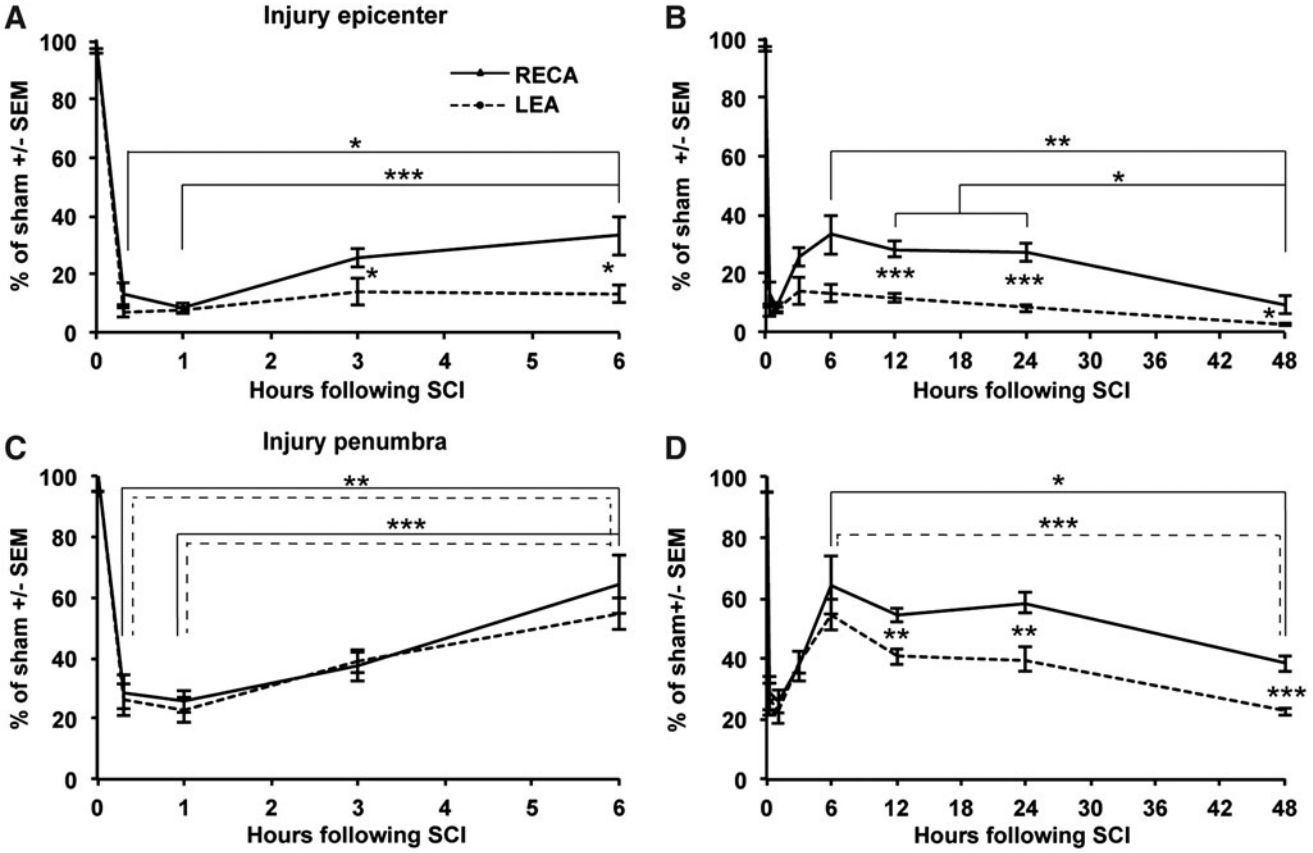

FIG. 2. Temporal changes in microvessel labeling reveals hypoperfusion following spinal cord contusion. The number of microvessels was counted in the two regions shown in Figure 1I at the injury epicenter and **(A,B)** and penumbra **(C,D)**. The data from **A** and **C** are also shown in **B** and **D**, but are presented separately to visualize all data during the acute injury phase. A rapid drop of LEA+ microvessels remains low at the epicenter **(A,B)**, whereas the perfusion recovers partially in the penumbra **(C,D)**. The difference between LEA and RECA as a general marker for blood vessels suggests that a subset of vessels is not being perfused. Data are shown as average plus SEM. Group sizes are five per time point of injury and eight sham operated animals. The horizontal broken lines represent the *p* values for LEA and the solid lines represent those for RECA. Differences between LEA and RECA are indicated by asterisks between the two data points. $*p<0.05$; $**p<0.01$; $***p<0.001$ by ANOVA with Tukey's multiple comparison's test.

Intravenous (i.v.) $MgCl_2$ treatment improves microvasculature perfusion after SCI

At 24 h after the T9 contusion injury, animals infused with saline had fewer LEA+ than RECA+ microvessels in the combined epicenter and penumbra (52±5% vs. 36±4% of sham; $p<0.05$; Fig. 4A). Continuous i.v. infusion with $MgCl_2$ during a 24 h period resulted in a higher number of LEA+ microvessels (57±5% vs. 36±4% of sham in vehicle- treated group; $p<0.05$; Fig. 4A). Also, with $MgCl_2$ treatment, the number of LEA+ microvessels was equal to the number of RECA+ ones, suggesting that all surviving microvessels were perfused. At the epicenter, more RECA+ microvessels were seen with $MgCl_2$ (52±4% vs. 44±2% with vehicle; $p<0.05$; data not shown).

At 48 h, animals infused with saline had fewer LEA+ than RECA+ microvessels (19±4% vs. 36±4% of sham; $p<0.05$; Fig. 4A). Continuous i.v. infusion over the same period with $MgCl_2$ had protective effects on microcirculatory flow, with increased numbers of LEA+ microvessels (30±4% vs. 19±4%; $p<0.05$; Fig. 4A). However, the number of RECA+ microvessels was higher than that of the LEA+ ones, suggesting that a subset of the vessels were not perfused at this time. At 48 h, the $MgCl_2$ treatment may have been protective for microvessels, as more RECA+ vessels were counted in the penumbra (59±7% vs. 42±3% with vehicle; $p<0.05$; data not shown).

Importantly, the increase in microcirculatory blood flow in response to the $MgCl_2$ treatment did not result in increased hemorrhage in epicenter or penumbra, as measured at 24 h (Fig. 4B).

MgCl2 treatment does not have neuroprotective effects

Motor neurons die through an excitotoxic mechanism following spinal cord contusion, and magnesium counteracts excitotoxicity in animal models of traumatic and hypoxic injury.[18,37–39] We therefore assessed ventral horn motor neuron survival at 24 h after injury in cresyl violet-stained sections. In both vehicle- and $MgCl_2$-infused animals, there was a total absence of motor neurons in the epicenter and at 1 mm from it (the penumbra), and we could not, therefore, count them. Compared with sham-operated rats (Fig. 5A), both vehicle- (Fig. 5B) and $MgCl_2$-infused animals (Fig. 5C), showed some survival of neurons in the ventral horn at 3 mm rostral from the injury epicenter. The number of motor neurons was not different in the vehicle- and $MgCl_2$-treated animals, being 21±2% and 20±3% of sham, respectively ($p>0.05$). Moreover, there was also loss of APC-positive oligodendrocytes in the ventral white matter at 3 mm rostral from the epicenter Fig. 5D–I). In sections

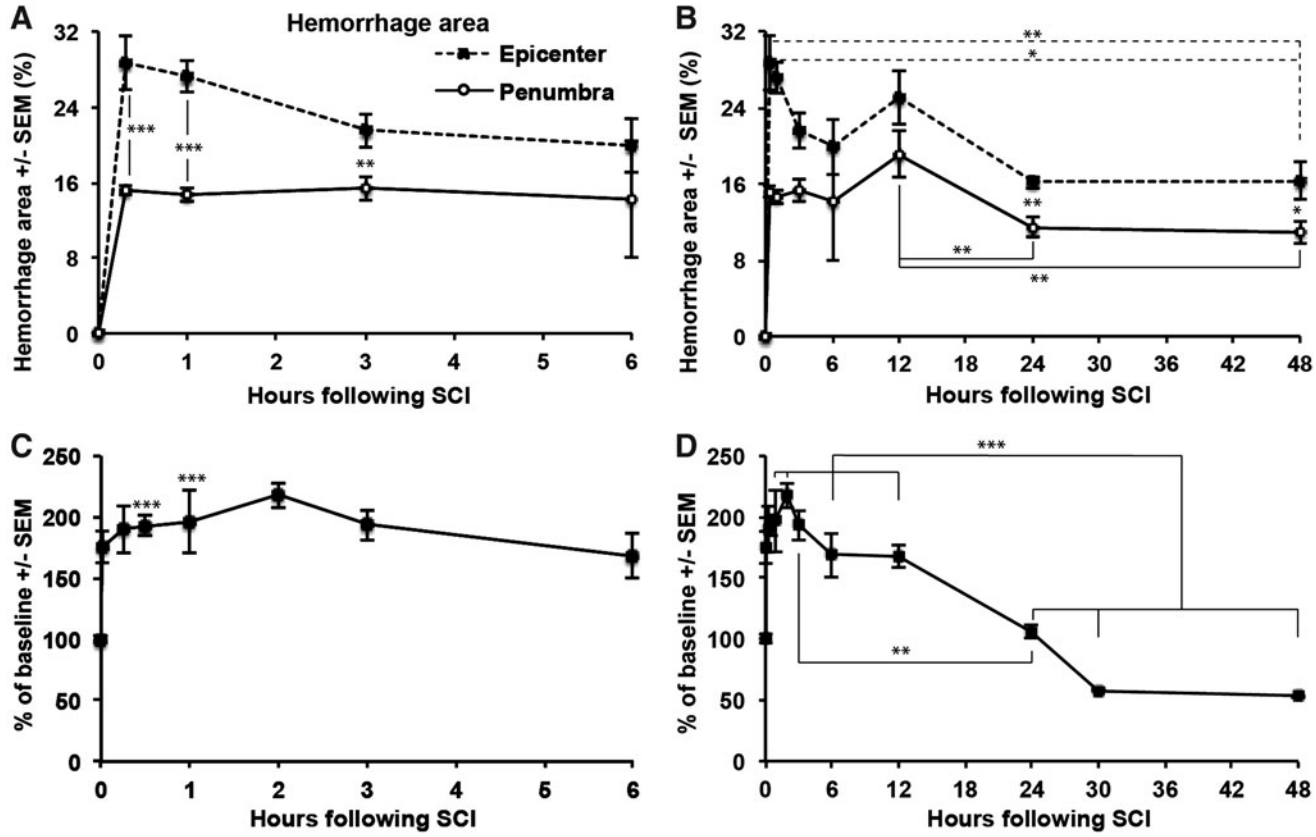

FIG. 3. Hemorrhage and peri-spinal cord hyperemia occurs rapidly following spinal cord contusion. **(A,B)** The area of diaminobenzidine (DAB) staining for hemorrhage in the epicenter and penumbra of injured cord were quantified. At 20 min, the hemorrhage area was already maximal, and it decreased by 24 h, perhaps because of hemolysis. Rats are the same as in Figure 2. ($*p<0.05$; $**p<0.01$; $***p<0.001$). **(C,D)** Doppler readings over the dorsal surface of the spinal cord with the sensor located just rostral to the injury epicenter were performed on a different set of rats. Each rat served as its own control; with 0 h values taken from immediately before the injury, and with measurements repeated over 48 h. $n=4$ rats. There is a rapid increase at 1 min after the injury with stable high values up to 12 h and decreasing flow to $\sim$50% of normal at 48 h ($***p<0.001$).

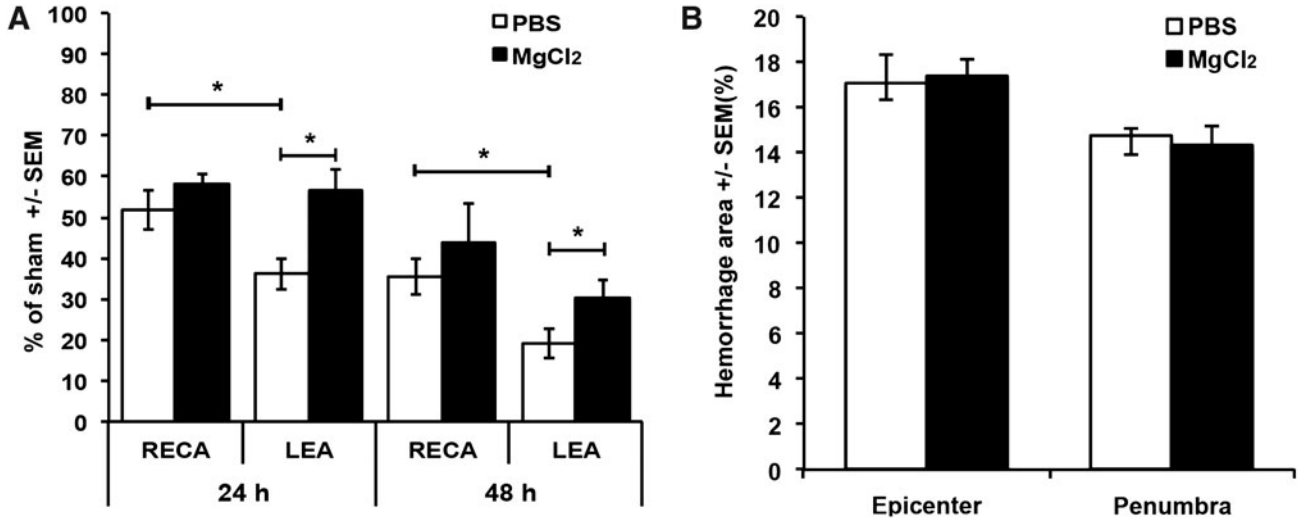

FIG. 4. Intravenous (i.v.) $MgCl_2$ treatment increased microvascular perfusion without increasing hemorrhage following spinal cord injury. **(A)** Shown are the percentages of RECA+ or LEA+ microvessels in the epicenter plus penumbra at 24 and 48 h. As shown also in a separate experiment (Fig. 2), the control phosphate-buffered saline (PBS)-treated animals displayed hypoperfusion status (LEA lower than RECA). The vasodilatory effect of $MgCl_2$ is still seen at 48 h, but the total number of microvessels is less than at 24 h. **(B)** There is no change in the area of hemorrhage with the $MgCl_2$ treatment at 24 h post-injury. $n=5$ per group. $*p<0.05$.

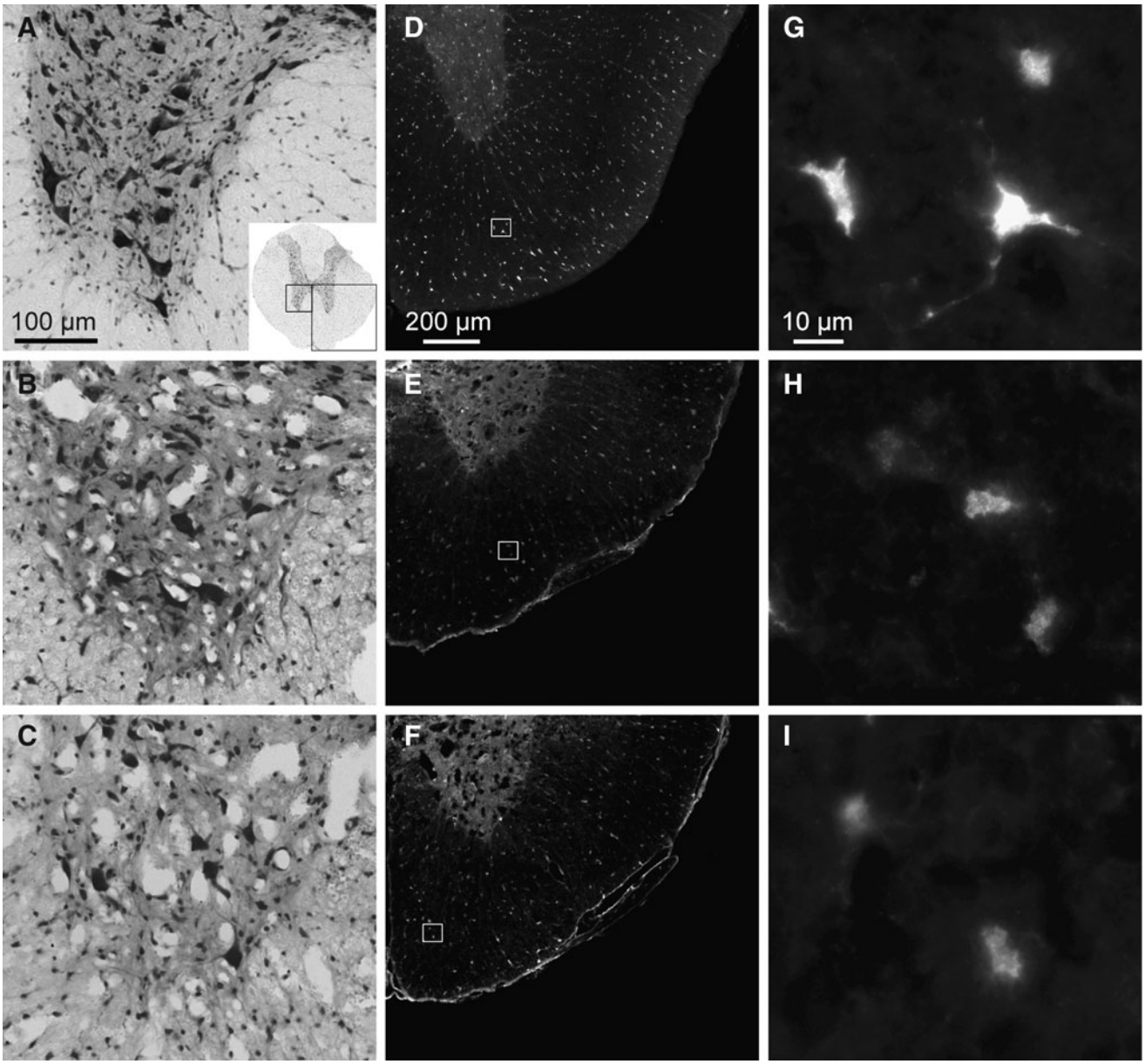

FIG. 5. $MgCl_2$ treatment does not protect motor neurons or oligodendrocytes after spinal cord injury. **(A)** A transverse section through the thoracic spinal cord of a sham-operated rat stained with cresyl violet clearly shows neuronal cell bodies, particularly the large somatic motor neurons of the ventral horn. The boxes in the inset indicate areas of ventral horn (left) and white matter (right) shown in **A–C** and **D–F** and which were used for quantification of neurons and oligodendrocytes. Scale bar = 100 μm. **(B)** With intravenous infusion of phosphate-buffered saline (PBS), fewer neurons are seen at 24 h after the contusion at 3 mm from the injury epicenter. **(C)** $MgCl_2$-treated rats also have fewer neurons. **(D)** APC-positive oligodendrocytes are equally distributed in the ventral white matter as shown in a transverse section from a sham-operated rat. Scale bar = 200 μm. **(E)** With intravenous infusion of PBS over 24 h following a contusive injury, fewer oligodendrocytes are seen at 3 mm from the injury epicenter. **(F)** $MgCl_2$-treated rats also have fewer oligodendrocytes. **(G–I)** Higher magnification images of **D–F**. Scale bar = 10 μm.

adjacent to those used for motor neuron counts, the percentage of APC-positive oligodendrocytes in the ventral white matter was not different, with $30 \pm 1\%$ and $35 \pm 3\%$ of sham seen in vehicle and $MgCl_2$ treated rats, respectively ($p > 0.05$). Therefore, despite the improved blood flow, the continuous infusion of $MgCl_2$ did not have neuroprotective or toxic effects during the acute injury phase.

We tested whether a 7-day i.v. treatment with $MgCl_2$ would have neuroprotective effects following the T9 contusion. Functional recovery, as measured by weekly BBB (Fig. 6A) and grid walk (Fig. 6B) tests, was not affected positively or negatively by the treatment, as the groups did not differ significantly. There was also no difference in white matter sparing at the epicenter ($48 \pm 3\%$ vs. $51 \pm 4\%$ of total cord area; Fig. 6C–E). There also was no difference between the number of LEA+ and RECA+ microvessels in the injury epicenter and penumbra (Fig. 6F).

Discussion

Our results show that contused spinal cord tissue undergoes rapid and severe hypoperfusion, which is partially restored over a

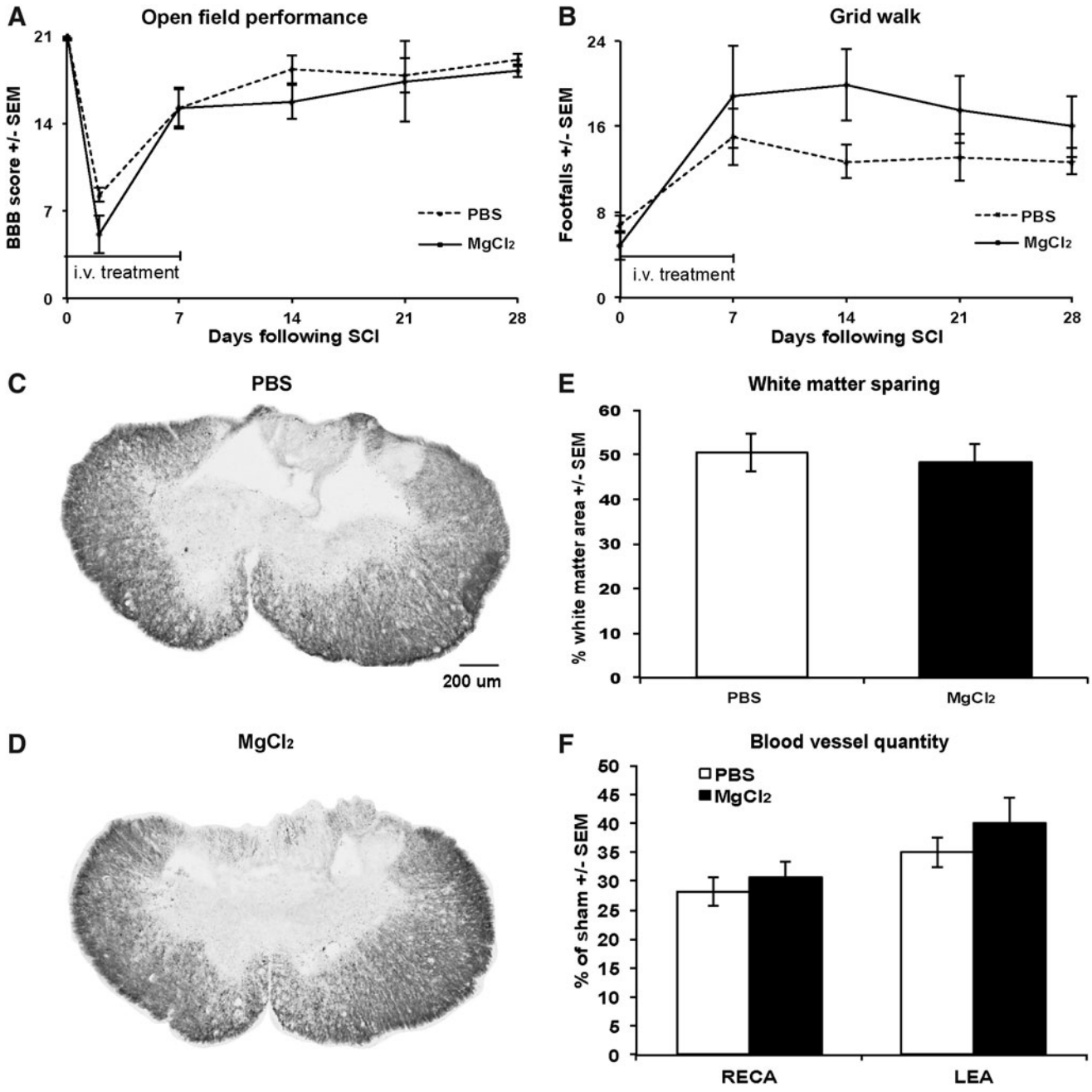

FIG. 6. Locomotor function, white matter sparing, and microvessel quantity is not affected by a 7 day intravenous (i.v.) $MgCl_2$ treatment following spinal cord injury. **(A)** The Basso–Beattie–Breshnahan (BBB) score for overground locomotor function is not different in the vehicle phosphate-buffered saline (PBS) and $MgCl_2$ treated groups over a 4 week period. **(B)** Grid walk performance is also not significantly different. **(C,D)** Examples of Eriochrome Cyanine (EC)-stained transverse sections at the epicenter in control PBS **(C)** and $MgCl_2$ **(D)** treated rats show the same extent of white matter sparing at 4 weeks as quantified in **(E)**. **(F)** In the same rats, the average percentage of RECA- and LEA-stained microvessels was not different. $n = 6$ for PBS and 5 for $MgCl_2$.

24 h period and can be improved by a clinically relevant i.v. infusion of $MgCl_2$. Blood flow disturbances, including vasospasm, after SCI have been studied before.[2,5,6,40,41] This study advances insight by microscopically analyzing microvascular blood flow using LEA lectin labeling, which identifies perfused microvessels lined with endothelial cells. We also extended previous data by focusing on the temporal changes during the earliest post-injury phase.

Microvascular perfusion at the epicenter was already greatly reduced to a minimum at the first time point 20 min following contusion. The discrepancy between LEA and the endothelial marker RECA suggested that a subset of microvessels remains unperfused by blood. Our finding that $MgCl_2$ causes increased perfusion suggests that the contusion induces vasospasm and hypoperfusion of the spinal cord parenchyma. The Doppler data showed an increase in blood flow during the first 12 h post-injury. This might be attributed to increased velocity after incomplete spasm of the extrinsic arteries on the posterior surface of the cord, which is consistent with the observations that they remain

patent.[1,41] Therefore, the microvascular hypoperfusion is most likely caused by spasm of the penetrating vessels. Capillaries themselves do not have smooth muscle cells that regulate perfusion of the microvascular network arterioles.[42] We do note that laser Doppler is considered less accurate for evaluating spinal cord blood flow than more invasive methods, such as hydrogen clearance or oxygen tension measurements.[11,43,44] Laser Doppler only provides an indirect measurement of actual blood flow in the spinal cord and does not directly measure capillary flow or oxygen levels in the parenchyma. The advantage is the preservation of tissue integrity, excluding a tissue injury confound and allowing serial measurements over long periods. This feature has been used to perform spinal cord blood flow studies in experimental, as well in clinical settings.[45,46]

The hemorrhagic area, which was analyzed by DAB staining, was already maximal at 20 min post-injury at both the injury epicenter and the penumbra, which indicates the sudden character of post-traumatic hemorrhage in the SCI.[47,48] Microvascular spasm is known to develop as a result of the toxic effects of blood,[49] although the physical trauma to vessels themselves also might induce spasm.[50] Intracerebral hemorrhage causes a modest reduction of cerebral blood flow, whereas subdural hematoma substantially decreases cerebral blood flow.[51] Therefore, bleeding after SCI could cause blood vessels in the arachnoid membrane and/or the perforating vessels to constrict, as it does in subarachnoid hemorrhage.[52] The DAB precipitate is catalyzed by peroxidases in the red blood cells, including hemoglobin, and has been used as a sensitive method to document spontaneous intracranial hemorrhage.[32] By flushing blood from the main circulation before collecting the spinal cord, the DAB product represents extravascular blood in the parenchyma and within coagulated vessels. The advantage of this DAB staining method is the ability to document the spread as well as the density of the bleeding in different areas of the spinal cord. One limitation of this method is the fact that blood and hemoglobin undergo transformation over time,[53] such that the DAB staining does not inform about the toxic blood products. Another limitation is that the measurements are only approximations of the total amount of bleeding. Others have measured total content of hemoglobin in spinal cord extracts, which is likely more accurate, or immunohistochemistry for iron in injured segments.[22,54]

After the initial acute drop, the number of perfused microvessels identified by LEA labeling recovers in the penumbra up to ~60% of normal. This reversal in perfusion is not seen at the epicenter and may indicate the difference in severity of the injury or secondary degeneration in the penumbra. The differences might be the result of hemorrhage because of the greater hemorrhage at the epicenter. Hemorrhage is a major cause of secondary degeneration likely caused by the progressive breakdown of erythrocytes and their release of free hemoglobin and iron, which are neurotoxic.[2,35,55,56] *In vitro,* blood clots begin to dissolve and release free hemoglobin after 24 h,[57] but *in vivo* this may be faster. The percentage of unperfused microvessels was greater at the epicenter than at the penumbra, and loss of RECA+ vessels at 48 h was greater at the epicenter (see also[20,21]). Therefore, microvessels at the epicenter might die because they are not perfused over the 48 h period. The finding that the microvasculature as well as its perfusion decreases between 24 and 48 h also suggests that chronic hypoperfusion might contribute to microvascular regression. Lack of blood flow is known to cause regression in development and in tumors.[58,59] Alternatively, the inflammatory response as one of the main known contributors to progressive tissue loss could also play a role in progressive endothelial cell loss.[60–63] This would be supported by our finding that the LEA and RECA values in the penumbra at 48 h are similar to those at the epicenter at 6 h, which may indicate the development of a wave of the secondary injury from the epicenter to adjacent areas. The partial recovery suggests that there is a window of opportunity for treatment lasting up to 24 h, at least in this injury model. We have previously seen protective effects on blood vessels of treatments started 4 h after a contusive injury in rats and mice.[20,21]

The benefit of infusing magnesium salt to relieve vascular spasm of CNS vessels is that it has previously been used in experimental and clinical settings,[64–66] and intravenous magnesium is one of the options for therapy for CNS vasospasm.[15,16] Our dosing is in the range that is deemed tolerable in humans.[18,30] Our data show that $MgCl_2$ can improve microvascular perfusion after a contusive SCI. The extent of maintained perfusion was similar with 24 or 48 h infusions. Together, the known vasodilatory effects of $MgCl_2$ and resolution of the discrepancy between LEA and RECA staining, suggests that $MgCl_2$ acted by reducing vasoconstriction of penetrating vessels around the injury site. One of our concerns was that improved perfusion of damaged microvessels would exacerbate the injury-induced hemorrhage. Intravenous magnesium treatments are considered safe in clinical use and do not cause increased bleeding in patients with subarachnoid hemorrhage or other disorders, such as cardiac arrest or respiratory paralysis.[67–69] Our study extends this to SCI, as we did not see an increase in the area of hemorrhage at the epicenter or penumbra with the $MgCl_2$ treatment over 24 h.

The $MgCl_2$ treatment only restored the number of perfused microvessels up to ~60% of normal. Together with the RECA staining for endothelial cells, this suggests that perfusion cannot be maintained in a subset of vessels, or that the primary injury causes death of endothelial cells. Others have shown an acute loss of endothelial cells very soon after a contusive injury.[22,70] We have been able to rescue endothelialized microvessels in mice with a similar severity of injury, for example, with angiopoietin-1, but only up to ~40% at the epicenter. This suggests that there is a substantial primary loss of microvessels resulting from the initial mechanical injury, which cannot be prevented. If correct, this suggests that there might be a limit to the extent to which neuroprotective agents could benefit patients with SCI, as the selective rescue of blood vessels is so clearly related to the ultimate recovery in experimental models.[21,22]

Our data show that despite improved perfusion of the injured spinal cord following intravenous $MgCl_2$ treatment, there was no lasting benefit, either in acute motor neuron or oligodendrocyte survival, chronic functional outcomes, or white matter sparing. Others had also shown that the vasodilator nimodipine could improve blood flow in the compression-injured spinal cord, but that it was ineffective in providing permanent protection of function and tissue.[12,13] However, the lack of any protective effect by magnesium was somewhat surprising, as it is thought to have anti-excitotoxic properties, and neuronal loss after SCI is thought to be caused by excitotoxicity.[37,39,71–73] Magnesium has neuroprotective effects in experimental models of brain injury, rescuing neurons.[74] However, we did not see an effect on lower motor neuron or oligodendrocyte survival during the acute phase of injury (24 h), even at a distance from the epicenter where a proportion of these cells had survived. Repeated i.v. injections of magnesium improved lesion volume, although not locomotor function, following contusive SCI.[18,30] Our study is also in apparent contrast to the finding that two i.v. injections of magnesium within the first 6 h result in dorsal white matter sparing and a small improvement in locomotor function in rats with a compression injury.[17] The absence of a

behavioral effect in the contusion model ([18] and this study) raises the possibility that the differences are related to the type of injury. However, it is more likely that the plasma levels reached in our study are different because of the continuous i.v. infusions (total 31 mg/day/rat) versus bolus injections with higher doses (120 mg/rat in two injections at 15 min and 6 h post-injury).[17] Such bolus injections would reach higher peaks but would be excreted more rapidly.[67] Intravenous injection leads to a 20-fold increase of urinary excretion, with 75% being excreted during the infusion.[75] Because of the pharmacodynamic and kinetic differences, we do not view our study as a typical replication of the others.

Despite improved perfusion, the decrease in the number of microvessels between 24 and 48 h after SCI was not markedly affected by the $MgCl_2$ treatment. One potential explanation to consider is the proposed reperfusion injury following SCI.[24] The reduction seen between 24 and 48 h without the treatment might also be consistent with this idea. Therefore, it is possible that endothelial cells in reperfused microvessels need to be protected during the vasodilation in order to survive permanently. One such possible combination of vasodilator and endothelial protective agent might have been present in the combination of magnesium and polyethylene glycol.[18,30] The latter is a synthetic polymer, and reportedly has neuroprotective effects in acute SCI.[17,76,77] Its effects might be mediated by its ability to fuse cell membranes and this may include endothelial cells. We propose that maintaining or improving microvascular perfusion should enhance the bioavailability of any protective drug administered intravenously, whether it is intended to rescue endothelial cells, which is a very promising route, or other cells. The finding that magnesium has no obvious detrimental effects following SCI, also in this study, suggests that it would ultimately be safe in humans with SCI.

We use the well-characterized IH impactor, as it is one of the commonly used graded impactors in SCI field,[78] and it was the one used in by Kwon et al.[18] However, before extrapolating these data to humans with SCI, it should be noted that none of the existing contusion or compression injuries completely models the full range of changes occurring in human SCI, including the common burst fracture. In addition to longer dwell time in cases of compression and dislocation, there are other differences, such as the closed versus open injury, and the more common ventral injury versus the dorsal approach in experimental settings.

Collectively, our results suggest that vascular spasm causes dysfunction of microcirculatory blood flow early following SCI, and that many surviving microvessels are reperfused by 24 h, offering a window for therapeutic intervention. We also show that the clinically relevant continuous i.v. infusion of $MgCl_2$ can normalize perfusion in the surviving microvessels, opening up a new insight into how to improve access for neuroprotective agents to the injured spinal cord tissue.

Acknowledgments

We thank Rollie Reid (1972–2011), Yun Shi Long, Hillary Conway, Sheila Arnold, Christine Yarberry, Kim Cash, and Darlene Burke for their excellent technical assistance. This work was supported by a grant from the Kentucky Spinal Cord and Head Injury Trust, and by NS045734, GM103507, Norton Healthcare, and the Commonwealth of Kentucky Challenge for Excellence.

Author Disclosure Statement

No competing financial interests exist.

References

1. Koyanagi, I., Tator, C. H., and Theriault, E. (1993). Silicone rubber microangiography of acute spinal cord injury in the rat. Neurosurgery 32, 260–268.
2. Mautes, A. E., Weinzierl, M. R., Donovan, F., and Noble, L. J. (2000). Vascular events after spinal cord injury: contribution to secondary pathogenesis. Phys. Ther. 80, 673–687.
3. Benton, R. L., and Hagg, T. (2011). Vascular pathology as a potential therapeutic target in SCI. Transl. Stroke Res. 2, 556–574.
4. Fassbender, J. M., Whittemore, S. R., and Hagg, T. (2011). Targeting microvasculature for neuroprotection after SCI. Neurotherapeutics 8, 240–251.
5. Dohrmann, G. J., and Wick, K. M. (1971). Demonstration of the microvasculature of the spinal cord by intravenous injection of the fluorescent dye, thioflavine s. Stain Technol. 46, 321–322.
6. Dohrmann, G. J., and Allen, W. E. (1975). Microcirculation of traumatized spinal cord. A correlation of microangiography and blood flow patterns in transitory and permanent paraplegia. J Trauma 15, 1003–1013.
7. Guha, A., Tator, C. H., and Piper, I. (1985). Increase in rat spinal cord blood flow with the calcium channel blocker, nimodipine. J. Neurosurg. 63, 250–259.
8. Kobrine, A. I., Doyle, T. F., and Martins, A. N. (1975). Local spinal cord blood flow in experimental traumatic myelopathy. J. Neurosurg. 42, 144–149.
9. Balentine, J. D. (1978). Pathology of experimental spinal cord trauma. I. The necrotic lesion as a function of vascular injury. Lab. Invest. 39, 236–253.
10. Simard, J. M., Woo, S. K., Tsymbalyuk, N., Voloshyn, O., Yurovsky, V., Ivanova, S., Lee, R., and Gerzanich, V. (2012). Glibenclamide—10-h treatment window in a clinically relevant model of stroke. Transl. Stroke Res. 3, 286–295.
11. Fehlings, M. G., Tator, C. H., and Linden, R. D. (1989). The effect of nimodipine and dextran on axonal function and blood flow following experimental spinal cord injury. J. Neurosurg. 71, 403–416.
12. Guha, A., Tator, C. H., Smith, C. R., and Piper, I. (1989). Improvement in post-traumatic spinal cord blood flow with a combination of a calcium channel blocker and a vasopressor. J. Trauma 29, 1440–1447.
13. Ross, I. B., Tator, C. H., and Theriault, E. (1993). Effect of nimodipine or methylprednisolone on recovery from acute experimental spinal cord injury in rats. Surg. Neurol. 40, 461–470.
14. Pointillart, V., Petitjean, M. E., Wiart, L., Vital, J. M., Lassié, P., Thicoipé, M., and Dabadie, P. (2000). Pharmacological therapy of spinal cord injury during the acute phase. Spinal Cord 38, 71–76.
15. Zubkov, A. Y., and Rabinstein, A. A. (2009). Medical management of cerebral vasospasm: present and future. Neurol. Res. 31, 626–631.
16. Rabinstein, A. A., Lanzino, G., and Wijdicks, E. F. (2010). Multidisciplinary management and emerging therapeutic strategies in aneurysmal subarachnoid haemorrhage. Lancet Neurol. 9, 504–519.
17. Ditor, D. S., John, S. M., Roy, J., Marx, J. C., Kittmer, C., and Weaver, L. C. (2007). Effects of polyethylene glycol and magnesium sulfate administration on clinically relevant neurological outcomes after spinal cord injury in the rat. J. Neurosci. Res. 85, 1458–1467.
18. Kwon, B. K., Roy, J., Lee, J. H. T., Okon, E., Zhang, H., Marx, J. C., and Kindy, M. S. (2009). Magnesium chloride in a polyethylene glycol formulation as a neuroprotective therapy for acute spinal cord injury: preclinical refinement and optimization. J. Neurotrauma 26, 1379–1393.
19. Lee, J. S., Han, Y. M., Yoo, D. S., Choi, S. J., Choi, B. H., Kim, J. H., Kim, Y. H., Huh, P. W., Ko, Y. J., Rha, H. K., Cho, K. S., and Kim, D. S. (2004). A molecular basis for the efficacy of magnesium treatment following traumatic brain injury in rats. J. Neurotrauma 21, 549–561.
20. Nakashima, S., Arnold, S. A., Mahoney, E. T., Sithu, S. D., Zhang, Y. P., D'Souza, S. E., Shields, C. B., and Hagg, T. (2008). Small-molecule protein tyrosine phosphatase inhibition as a neuroprotective treatment after spinal cord injury in adult rats. J. Neurosci. 28, 7293–7303.
21. Han, S., Arnold, S. A., Sithu, S. D., Mahoney, E. T., Geralds, J. T., Tran, P., Benton, R. L., Maddie, M. A., D'Souza, S. E., Whittemore, S. R., and Hagg, T. (2010). Rescuing vasculature with intravenous angiopoietin-1 and alpha v beta 3 integrin peptide is protective after spinal cord injury. Brain 133, 1026–1042.
22. Simard, J. M., Tsymbalyuk, O., Ivanov, A., Ivanova, S., Bhatta, S., Geng, Z., Woo, S. K., and Gerzanich, V. (2007). Endothelial

sulfonylurea receptor 1–regulated ncca-atp channels mediate progressive hemorrhagic necrosis following spinal cord injury. J. Clin. Invest. 117, 2105–2113.
23. Carrico, K. M., Vaishnav, R., and Hall, E. D. (2009). Temporal and spatial dynamics of peroxynitrite-induced oxidative damage after spinal cord contusion injury. J. Neurotrauma 26, 1369–1378.
24. Guth, L., Zhang, Z., and Steward, O. (1999). The unique histopathological responses of the injured spinal cord. Implications for neuroprotective therapy. Ann. N. Y. Acad. Sci. 890, 366–384.
25. Noble, L. J., Mautes, A. E., and Hall, J. J. (1996). Characterization of the microvascular glycocalyx in normal and injured spinal cord in the rat. J. Comp. Neurol. 376, 542–556.
26. Thurston, G., Baluk, P., Hirata, A., and McDonald, D. M. (1996). Permeability-related changes revealed at endothelial cell borders in inflamed venules by lectin binding. Am. J. Physiol. 271, H2547–562.
27. Jilani, S. M., Murphy, T. J., Thai, S. N. M., Eichmann, A., Alva, J. A., and Iruela–Arispe, M. L. (2003). Selective binding of lectins to embryonic chicken vasculature. J. Histochem. Cytochem. 51, 597–604.
28. Mozer, A. B., Whittemore, S. R., and Benton, R. L. (2010). Spinal microvascular expression of pv-1 is associated with inflammation, perivascular astrocyte loss, and diminished ec glucose transport potential in acute sci. Curr. Neurovasc. Res. 7, 238–250.
29. Benton, R. L., Maddie, M. A., Minnillo, D. R., Hagg, T., and Whittemore, S. R. (2008). Griffonia simplicifolia isolectin b4 identifies a specific subpopulation of angiogenic blood vessels following contusive spinal cord injury in the adult mouse. J. Comp. Neurol. 507, 1031–1052.
30. Lee, J., Roy, J., Sohn, H. M., Cheong, M., and Liu, J. (2010). Magnesium in a polyethylene glycol formulation provides neuroprotection after unilateral cervical spinal cord injury. Spine 35, 2041–2048.
31. Basso, D. M., Beattie, M. S., and Bresnahan, J. C. (1996). Graded histological and locomotor outcomes after spinal cord contusion using the nyu weight-drop device versus transection. Exp. Neurol. 139, 244–256.
32. Wakisaka, Y., Miller, J. D., Chu, Y., Baumbach, G. L., Wilson, S., Faraci, F. M., Sigmund, C. D., and Heistad, D. D. (2008). Oxidative stress through activation of nad(p)h oxidase in hypertensive mice with spontaneous intracranial hemorrhage. J. Cereb. Blood Flow Metab. 28, 1175–1185.
33. Rabchevsky, A. G., Fugaccia, I., Sullivan, P. G., and Scheff, S. W. (2001). Cyclosporin a treatment following spinal cord injury to the rat: behavioral effects and stereological assessment of tissue sparing. J. Neurotrauma 18, 513–522.
34. Loy, D. N., Crawford, C. H., Darnall, J. B., Burke, D. A., Onifer, S. M., and Whittemore, S. R. (2002). Temporal progression of angiogenesis and basal lamina deposition after contusive spinal cord injury in the adult rat. J. Comp. Neurol. 445, 308–324.
35. Noble, L. J., and Wrathall, J. R. (1989). Correlative analyses of lesion development and functional status after graded spinal cord contusive injuries in the rat. Exp. Neurol. 103, 34–40.
36. Martin, N. A., Doberstein, C., Zane, C., Caron, M. J., Thomas, K., and Becker, D. P. (1992). Posttraumatic cerebral arterial spasm: transcranial doppler ultrasound, cerebral blood flow, and angiographic findings. J. Neurosurg. 77, 575–583.
37. Liu, D., Xu, G. Y., Pan, E., and McAdoo, D. J. (1999). Neurotoxicity of glutamate at the concentration released upon spinal cord injury. Neuroscience 93, 1383–1389.
38. Park, E., Velumian, A. A., and Fehlings, M. G. (2004). The role of excitotoxicity in secondary mechanisms of spinal cord injury: a review with an emphasis on the implications for white matter degeneration. J. Neurotrauma 21, 754–774.
39. Mami, A. G., Ballesteros, J., Mishra, O. P., and Delivoria–Papadopoulos, M. (2006). Effects of magnesium sulfate administration during hypoxia on ca(2+) influx and ip(3) receptor modification in cerebral cortical neuronal nuclei of newborn piglets. Neurochem. Res. 31, 63–70.
40. Dohrmann, G. J., Wick, K. M., and Bucy, P. C. (1973). Spinal cord blood flow patterns in experimental traumatic paraplegia. J. Neurosurg. 38, 52–58.
41. Tator, C. H., and Koyanagi, I. (1997). Vascular mechanisms in the pathophysiology of human spinal cord injury. J. Neurosurg. 86, 483–492.
42. Attwell, D., Buchan, A. M., Charpak, S., Lauritzen, M., Macvicar, B. A., and Newman, E. A. (2010). Glial and neuronal control of brain blood flow. Nature 468, 232–243.
43. Hall, E. D., Yonkers, P. A., Horan, K. L., and Braughler, J. M. (1989). Correlation between attenuation of posttraumatic spinal cord ischemia and preservation of tissue vitamin E by the 21-aminosteroid u74006f: evidence for an in vivo antioxidant mechanism. J. Neurotrauma 6, 169–176.
44. Hukuda, S., and Amano, K. (1980). Spinal cord tissue oxygen in experimental ischemia, compression, and central necrosis. Spine 5, 303–306.
45. Young, W. F., Tuma, R., and O'Grady, T. (2000). Intraoperative measurement of spinal cord blood flow in syringomyelia. Clin. Neurol. Neurosurg. 102, 119–123.
46. Thompson, M. K., Tuma, R. F., and Young, W. F. (1999). The effects of pentoxifylline on spinal cord blood flow after experimental spinal cord injury. J. Assoc. Acad. Minor. Phys. 10, 23–26.
47. Sasaki, S. (1982). Vascular change in the spinal cord after impact injury in the rat. Neurosurgery 10, 360–363.
48. Choo, A. M., Liu, J., Lam, C. K., Dvorak, M., Tetzlaff, W., and Oxland, T. R. (2007). Contusion, dislocation, and distraction: primary hemorrhage and membrane permeability in distinct mechanisms of spinal cord injury. J. Neurosurg. Spine 6, 255–266.
49. Kolias, A. G., Sen, J., and Belli, A. (2009). Pathogenesis of cerebral vasospasm following aneurysmal subarachnoid hemorrhage: putative mechanisms and novel approaches. J. Neurosci. Res. 87, 1–11.
50. Alford, P. W., Dabiri, B. E., Goss, J. A., Hemphill, M. A., Brigham, M. D., and Parker, K. K. (2011). Blast-induced phenotypic switching in cerebral vasospasm. Proc. Natl. Acad. Sci. 108, 12,705–12,710.
51. Patel, T. R., Schielke, G. P., Hoff, J. T., Keep, R. F., and Lorris Betz, A. (1999). Comparison of cerebral blood flow and injury following intracerebral and subdural hematoma in the rat. Brain Res. 829, 125–133.
52. Krishna, V., Lazaridis, C., Ellegala, D., Glazier, S., Kindy, M., Spampinato, M., and Chalela, J. A. (2012). Spinal cord infarction associated with subarachnoid hemorrhage. Clin. Neurol. Neurosurg. 114, 1030–1032.
53. Del Bigio, M. R., Yan, H. J., Buist, R., and Peeling, J. (1996). Experimental intracerebral hemorrhage in rats. Magnetic resonance imaging and histopathological correlates. Stroke 27, 2312–2320.
54. Rathore, K. I., Kerr, B. J., Redensek, A., López–Vales, R., Jeong, S. Y., Ponka, P., and David, S. (2008). Ceruloplasmin protects injured spinal cord from iron-mediated oxidative damage. J. Neurosci. 28, 12,736–12,747.
55. Huang, F.-P., Xi, G., Keep, R. F., Hua, Y., Nemoianu, A., and Hoff, J. T. (2002). Brain edema after experimental intracerebral hemorrhage: role of hemoglobin degradation products. J. Neurosurg. 96, 287–293.
56. Nakamura, T., Keep, R. F., Hua, Y., Hoff, J. T., and Xi, G. (2005). Oxidative DNA injury after experimental intracerebral hemorrhage. Brain Res. 1039, 30–36.
57. Jaremko, K. M., Chen–Roetling, J., Chen, L., and Regan, R. F. (2010). Accelerated hemolysis and neurotoxicity in neuron-glia-blood clot cocultures. J. Neurochem. 114, 1063–1073.
58. Norden, A. D., Drappatz, J., and Wen, P. Y. (2008). Novel antiangiogenic therapies for malignant gliomas. Lancet Neurol. 7, 1152–1160.
59. Augustin, H. G., Young Koh, G., Thurston, G., and Alitalo, K. (2009). Control of vascular morphogenesis and homeostasis through the angiopoietin–tie system. Nat. Rev. Mol. Cell Biol. 10, 165–177.
60. Popovich, P. G., Guan, Z., Wei, P., Huitinga, I., van Rooijen, N., and Stokes, B. T. (1999). Depletion of hematogenous macrophages promotes partial hindlimb recovery and neuroanatomical repair after experimental spinal cord injury. Exp. Neurol. 158, 351–365.
61. Weaver, L. C., Gris, D., Saville, L. R., Oatway, M. A., Chen, Y., Marsh, D. R., Hamilton, E. F., and Dekaban, G. A. (2005). Methylprednisolone causes minimal improvement after spinal cord injury in rats, contrasting with benefits of an anti-integrin treatment. J. Neurotrauma 22, 1375–1387.
62. Donnelly, D. J., and Popovich, P. G. (2008). Inflammation and its role in neuroprotection, axonal regeneration and functional recovery after spinal cord injury. Exp. Neurol. 209, 378–388.
63. Pineau, I., Sun, L., Bastien, D., and Lacroix, S. (2010). Astrocytes initiate inflammation in the injured mouse spinal cord by promoting the entry of neutrophils and inflammatory monocytes in an il-1 receptor/myd88-dependent fashion. Brain Behav. Immun. 24, 540–553.
64. Stippler, M., Crago, E., Levy, E. I., Kerr, M. E., Yonas, H., Horowitz, M. B., and Kassam, A. (2006). Magnesium infusion for vasospasm

prophylaxis after subarachnoid hemorrhage. J. Neurosurgery 105, 723–729.
65. Mori, K., Miyazaki, M., Iwata, J., Yamamoto, T., and Nakao, Y. (2008). Intracisternal infusion of magnesium sulfate solution improved reduced cerebral blood flow induced by experimental subarachnoid hemorrhage in the rat. Neurosurg. Rev. 31, 197–203.
66. Westermaier, T., Stetter, C., Vince, G. H., Pham, M., Tejon, J. P., Eriskat, J., Kunze, E., Matthies, C., Ernestus, R.-I., Solymosi, L., and Roosen, K. (2010). Prophylactic intravenous magnesium sulfate for treatment of aneurysmal subarachnoid hemorrhage: a randomized, placebo-controlled, clinical study. Crit. Care Med. 38, 1284–1290.
67. Lu, J. F. and Nightingale, C. H. (2000). Magnesium sulfate in eclampsia and pre-eclampsia: pharmacokinetic principles. Clin. Pharmacokinet. 38, 305–314.
68. van Norden, A. G. W., van den Bergh, W. M., and Rinkel, G. J. E. (2005). Dose evaluation for long-term magnesium treatment in aneurysmal subarachnoid haemorrhage. J. Clin. Pharm. Ther. 30, 439–442.
69. Lameris, A. L., Monnens, L. A., Bindels, R. J., and Hoenderop, J. G. J. (2012). Drug-induced alterations in mg2+ homoeostasis. Clin. Sci. (Lond.) 123, 1–14.
70. Casella, G. T. B., Bunge, M. B., and Wood, P. M. (2006). Endothelial cell loss is not a major cause of neuronal and glial cell death following contusion injury of the spinal cord. Exp. Neurol. 202, 8–20.
71. Farooque, M., Hillered, L., Holtz, A., and Olsson, Y. (1996). Changes of extracellular levels of amino acids after graded compression trauma to the spinal cord: an experimental study in the rat using microdialysis. J. Neurotrauma 13, 537–548.
72. Zhang, L., Rzigalinski, B. A., Ellis, E. F., and Satin, L. S. (1996). Reduction of voltage-dependent mg2+ blockade of nmda current in mechanically injured neurons. Science 274, 1921–1923.
73. McAdoo, D. J., Xu, G., Robak, G., Hughes, M. G., and Price, E. M. (2000). Evidence that reversed glutamate uptake contributes significantly to glutamate release following experimental injury to the rat spinal cord. Brain Res. 865, 283–285.
74. Saatman, K. E., Bareyre, F. M., Grady, M. S., and McIntosh, T. K. (2001). Acute cytoskeletal alterations and cell death induced by experimental brain injury are attenuated by magnesium treatment and exacerbated by magnesium deficiency. J. Neuropathol. Exp. Neurol. 60, 183–194.
75. Cruikshank, D. P., Pitkin, R. M., Donnelly, E., and Reynolds, W. A. (1981). Urinary magnesium, calcium, and phosphate excretion during magnesium sulfate infusion. Obstet. Gynecol. 58, 430–434.
76. Duerstock, B. S., and Borgens, R. B. (2002). Three-dimensional morphometry of spinal cord injury following polyethylene glycol treatment. J. Exp. Biol. 205, 13–24.
77. Koob, A. O., Duerstock, B. S., Babbs, C. F., Sun, Y., and Borgens, R. B. (2005). Intravenous polyethylene glycol inhibits the loss of cerebral cells after brain injury. J. Neurotrauma 22, 1092–1111.
78. Scheff, S. W., Rabchevsky, A. G., Fugaccia, I., Main, J. A., and Lumpp, J. E. (2003). Experimental modeling of spinal cord injury: characterization of a force-defined injury device. J. Neurotrauma 20, 179–193.

Address correspondence to:
Theo Hagg, MD, PhD
Kentucky Spinal Cord Injury Research Center
511 South Floyd Street
MDR Building, Room 616
Louisville, KY 40292

E-mail: theo.hagg@louisville.edu